Ion-Driven ATP Pump by Self-Organized Hybrid Membrane Materials

ARTICLE *in* JOURNAL OF THE AMERICAN CHEMICAL SOCIETY · APRIL 2004

Impact Factor: 12.11 · DOI: 10.1021/ja039146z · Source: PubMed

J|A|C|S
ARTICLES
Published on Web 02/28/2004

Ion-Driven ATP Pump by Self-Organized Hybrid Membrane Materials

Mihail Barboiu,*,† Sophie Cerneaux,† Arie van der Lee,† and Gavin Vaughan‡

Contribution from the Institut Européen des Membranes, CNRS 5635, Place Eugène Bataillon, CC 47, F-34095 Montpellier, Cedex 5, France, and European Synchrotron Radiation Facility, BP 220, 38043, Grenoble Cedex France

Received October 21, 2003; E-mail: barboiu@iemm.univ-montp2.fr

Abstract: We report new hybrid organic−inorganic materials, based on macrocyclic receptors **1**−**3** self-organized in tubular superstructures prepared by sol−gel process. Fourier transform infrared (FTIR) and NMR spectroscopic analyses demonstrate that the self-organization by hydrogen bonding of organogel superstructures of **2** and **3** were preserved in the hybrid materials throughout the sol−gel process. The molecular arrangement of heteroditopic receptors defines a particularly attractive functional transport device for both cation (tubular macrocycles) and anion (sandwich-urea) directional-diffusion transport mechanism in the hybrid membrane material. This system has been employed successfully to design a *solid dense membrane*, functioning as an ion-powered adenosine triphosphate (ATP^{2-}) pump, and illustrates how a self-organized hybrid material performs interesting and potentially useful functions.

Molecular self-organization and the self-assembly to supramolecular structures is the basis for the construction of new functional nanomaterials in a bottom-up strategy. The way from molecular to nano(micro)scale devices depends both on the nature of its constituents and on the interactions between them.[1] Hybrid organic−inorganic materials produced by sol−gel processes are the subject of various investigations, offering the opportunity to achieve nanostructured materials first from molecular[2] or more recently from self-organized supramolecular[3] silsesquioxane systems.

The field of *hybrid supramolecular materials* covers all materials whose silsesquioxane precursors are initially connected through weak reversible noncovalent interactions so that they spontaneously undergo dynamic self-assembly and disassembly processes. This feature confers dynamic character on structure-directing supramolecular aggregates and resulted hybrid materials could incorporate defects on their sol−gel transcription, which can be expressed differently in response to external or environmental factors such as solvent, temperature, catalyst, etc. A rational approach to such functional hybrid nanomaterials requires mastering the competing dynamic interactions and hierarchical phase organizations between the dynamic self-assembly of organic moieties via noncovalent weak interactions and the rigid siloxane network formation via strong covalent bonds.[2,3]

Of special interest is *structure-directed function of hybrid materials* and control of their build-up from suitable units by self-organization. Toward this objective, our aim is to develop *functional hybrid membrane materials* that form selective patterns so as to enable efficient translocation events. Artificial systems, functioning as carriers or as channel-forming superstructures in liquid and bilayer membranes, are extensively developed.[4] We searched for hybrid solid membranes in which the molecular recognition-driven transport function could be ensured by a well-defined incorporation of specific organic receptors, covalently linked in a dense siloxane inorganic matrix. Of particular interest are the mechanical stability and the potential ability of such thin-layer solid membrane films to present functional properties such as solute molecular recognition and possibly generation of the directional conduction pathways by self-assembling at the supramolecular level.[5,6]

† Institut Européen des Membranes.
‡ European Synchrotron Radiation Facility.

(1) (a) Lehn, J.-M. *Supramolecular Chemistry-Concepts and Perspectives*; VCH: Weinheim, Germany, 1995. (b) Lehn, J.-M. *Chem. Eur. J.* **1999**, *5*, 2455−2463.
(2) (a) Terech, P.; Weiss, R. G. *Chem. Rev.* **1997**, 3133−3160. (b) Abdallah, D. J.; Weiss, R. G. *Adv. Mater.* **2000**, *12*, 1237−1247. (c) Corriu, R. J. P. *Eur. J. Inorg. Chem.* **2001**, *5*, 1109−1121. (d) Boury, B.; Corriu, R. J. P. *Chem. Rec.* **2003**, *2*, 120−132. (e) Sanchez, C.; Soler-Ilia, G. J. de A. A.; Ribot, F.; Lalot, T.; Mayer, C. R.; Cabuil, V. *Chem Mater.* **2001**, *13*, 3061−3083.
(3) (a) van Bommel, K. J. C.; Frigerri, A.; Shinkai, S. *Angew. Chem., Int. Ed.* **2003**, *42*, 980−999. (b) Moreau, J. J. E.; Velutini, L.; Wong, C.-M. M.; Bied, C. *Chem. Eur. J.* **2003**, *9*, 1594−1599. (c) Moreau, J. J. E.; Velutini, L.; Wong C.-M. M.; Bied, C.; Dieudonne, P.; Bantignes, J.-L. *J. Am. Chem. Soc.* **2001**, *123*, 7957−7958.
(4) (a) Gokel, G. W.; Mukhopadhyay, A. *Chem. Soc Rev.* **2001**, *30*, 274−286. (b) Voyer, N. *Top. Curr. Chem.* **1996**, *184*, 1−35. (c) Bong, D. T.; Clark, T. D.; Granja, J. R.; Ghadiri, M. R. *Angew. Chem., Int. Ed.* **2001**, *40*, 988−1011. (d) Mantile, S. *Chem. Soc Rev.* **2001**, *30*, 158−167.
(5) (a) Begin, U.; Zipp, G.; Möller, M. *Adv. Mater.* **2000**, *12*, 510−513. (b) Noble, R. D. *J. Chem. Soc., Faraday Trans.* **1991**, *87*, 2089−2092. (c) Thunhorst, K. L.; Noble, R. D.; Bowman, C. N. *Polym. Mater. Sci. Eng.* **1997**, *77*, 280−281. (d) Cussler, E. L.; Aris, R.; Brown, A. *J. Membr. Sci.* **1989**, *43*, 149−164.
(6) (a) Barboiu, M.; Luca, C.; Guizard, C.; Hovnanian, N.; Cot, L.; Popescu, G. *J. Membr. Sci.* **1997**, *129*, 197−207. (b) Barboiu, M.; Guizard, C.; Luca, C.; Albu, B.; Hovnanian, N.; Palmeri, J. *J. Membr. Sci.* **1999**, *161*, 193−206. (c) Barboiu, M.; Guizard, C.; Hovnanian, N.; Palmeri, J.; Reibel, C.; Luca, C.; Cot, L. *J. Membr. Sci.* **2000**, *172*, 91−103. (d) Barboiu, M.; Guizard, C.; Luca, C.; Hovnanian, N.; Palmeri, J.; Cot, L. *J. Membr. Sci.* **2000**, *174*, 277−286. (e) Barboiu, M.; Guizard, C.; Hovnanian, N.; Cot, L. *Sep. Technol. Pur.* **2001**, *25*, 211−218. (f) Lacan, P.; Guizard, C.; Le Gall, P.; Wettling, D.; Cot, L. *J. Membr. Sci.* **1995**, *100*, 99−109.

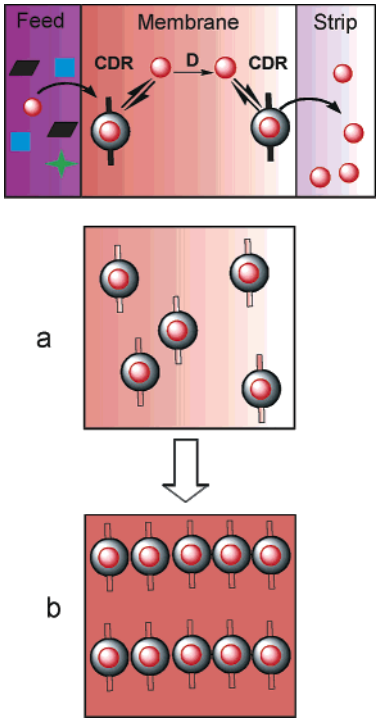

Figure 1. Assisted-diffusion mechanism of the solute by complexation−decomplexation reactions in solid dense fixed-site complexant membranes (D, diffusion; CDR, complexation−decomplexation reactions):[5] (a) first generation of randomly ordered molecular recognition-based membranes;[6] (b) second generation of self-organized fixed-site complexant membranes.

We have recently designed the first generation of thin-layer hybrid membranes,[6] based on polytopic macrocyclic receptors, randomly dispersed in a hybrid silica matrix. They are based on the incorporation of suitable instructions into molecular components, for the multiple recognition transport-based functions. In these *fixed-site complexant membranes* the fixed receptor is not a carrier; it just selectively assists the solute diffusion (D) in the membrane by selective complexation−decomplexation reactions (CDR) at the receptor-site level (Figure 1). It results in a new hybrid membrane system in which the "fixed-site jumping" diffusion[5b,c] of solutes into the dense silica material is controlled by the specific interactions with the fixed receptor and by the ion-induced diffusion phenomena (Figure 1a).[6] In nature, biological pore proteins represent an excellent example of structure-directed transport function. Proteins rely on various combinations of their molecular information to control ionic diffusion along polar transduction pathways.[7] This same premise hold true for suitably designed thin-layer hybrid membranes, minimizing the distance between the receptors by self-organization, with the hope to reduce the nonselective solute diffusion (D) and to create functional favorable diffusion patterns for the mobile solute into the solid dense material (Figure 1b).

Here we report new hybrid organic−inorganic materials, based on macrocyclic receptors **1**−**3** self-organized in tubular superstructures. These self-organized hybrid membrane materials, prepared by sol−gel processes, transport adenosine triphosphate (ATP^{2-}) anions upon a synthetic ion-driven pump "fueled" by a Na^+ concentration gradient.

(7) Hucho, F.; Weise, C. *Angew. Chem., Int. Ed.* **2001**, *40*, 3100−3116.

Chart 1

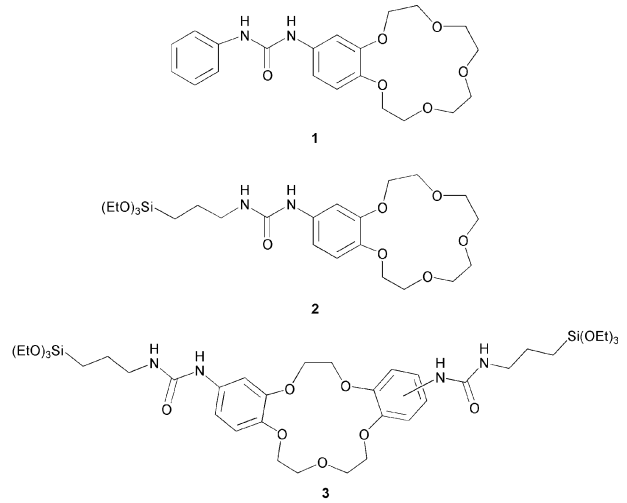

The hierarchical generation of such functional hybrid materials has been realized in two steps. First, the self-assembling properties of **1**−**3** in the aprotic solvents were analyzed, revealing the formation of supramolecular oligomers. They generate organogels in chloroform, leading in a second *sol*−*gel transcription* (polymerization) step to lamellar solid hybrid membrane materials at nanoscopic scale.

Three heteroditopic macrocyclic receptors **1**−**3** were prepared for the studies described here (Chart 1). They generate self-organized tubular superstructures[12] in solution and in the solid state based on three encoded features: (1) molecular recognition sites for the anion and the cation are covalently linked;[8] (2) the supramolecular guiding interaction is the urea head-to-tail H-bond association,[9a] assisted by $\pi-\pi$ stacking interactions (Figure 2a,b); and (3) the covalently bonded triethoxysilyl groups allow us, by sol−gel processes, to transcribe (to freeze) the solution self-organized dynamic superstructures in a solid heteropolysiloxane material (Figure 2c).

^{1}H NMR dilutions experiments on solutions of **1**−**3** showed a strong downfield shift of both NH protons[10] upon increasing the concentration in $CDCl_3$, which is indicative of self-association through intermolecular H-bonding. The association of **1**−**3** could be described with a cooperative association model[11,12] and indicates that higher aggregates were formed. This method assumes that all but the first equilibrium constant K_2, describing dimerization, are the same K_a and gives the association constants shown in Table 1.

We have found by variable-temperature ^{1}H NMR[10] that the association process of **1** is driven by enthalpy ($\Delta H_2 = -14.3$ kJ/mol, $\Delta H_a = -27.4$ kJ/mol), which is sufficient to overcome an increasing entropy barrier [$\Delta S_2 = -9.1$ J/(mol·K), $\Delta S_a = -27.4$ J/(mol·K)].[12] The formation of larger aggregates is

(8) Scheerder, J.; Duynhoven, J. P. M.; Engbersen, J. F. J.; Reinhoudt, D. N. *Angew. Chem., Int. Ed. Engl.* **1996**, *35*, 1090−1093.
(9) (a) Etter, M. C. *Acc. Chem. Res.* **1990**, *23*, 120−126. (b) Janiak, C. *J. Chem. Soc., Dalton Trans.* **2000**, 3885−3896.
(10) Equilibration between hydrogen-bonded and non-hydrogen-bonded states for a given N−H proton is almost always fast on the NMR time scale, and observed proton chemical shifts are weighted averages of the chemical shifts of contributing states. Variable-temperature NH proton experiments were performed for **1** in the range of 253−298 K.
(11) (a) Akiama, M.; Ohtani, T. *Spectrochim. Acta* **1994**, *50A*, 317−324. (b) de Loos, M.; van Esch, J.; Kellog, R. M.; Feringa, B. L. *Angew. Chem., Int. Ed.* **2001**, *40*, 613−616.
(12) Barboiu, M.; Vaughan, G.; van der Lee, A. *Org. Lett.* **2003**, *5*, 3073−3076.

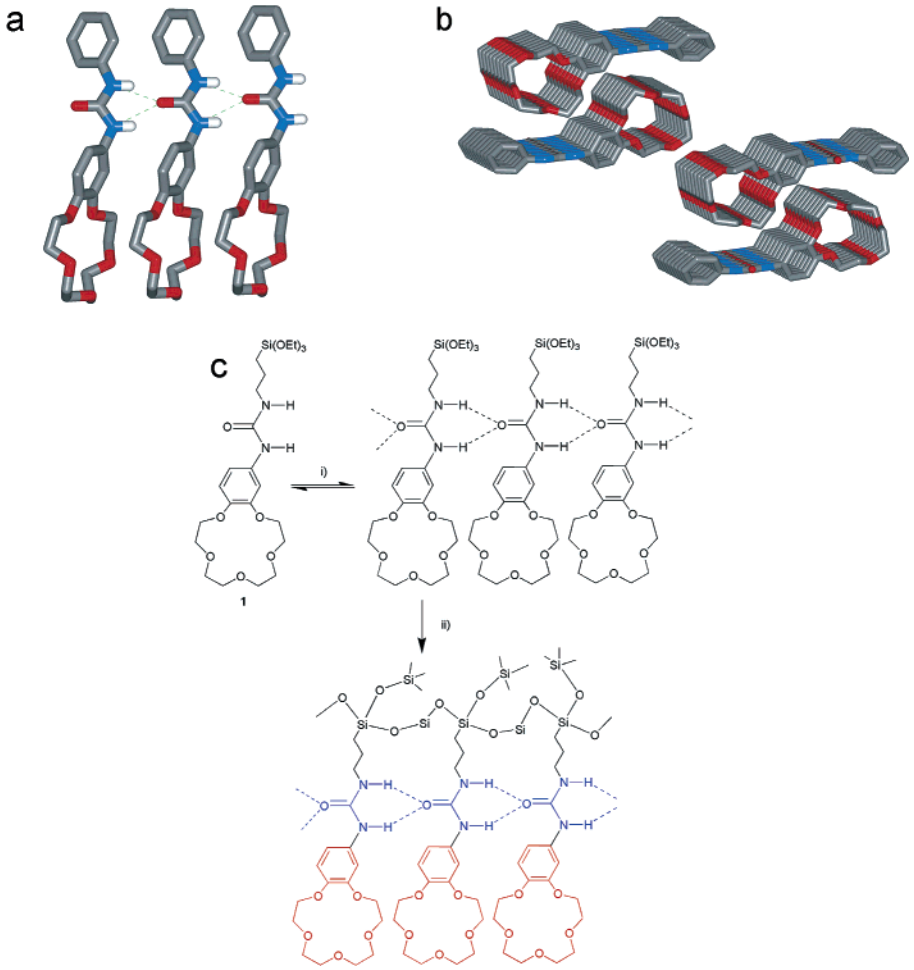

Figure 2. Crystal structure of macrocyclic receptor **1**. (a) Stick representation of H-bond superstructures. (b) CPK representation of the packing of **1** in the crystal.[12] (c) Schematic representation of the hierarchical generation: (i) self-organization in solution and (ii) sol−gel transcription of encoded molecular features into a hybrid heteropolysiloxane material.

Table 1. Calculated Association Constants of **1**−**3** and Downfield Shifts from ^{1}H NMR Experiments[a]

compd	K_2 (M^{-1})	K_a (M^{-1})	$\Delta\delta_{obs}$ [b] (ppm)	C_{max} [c] (M)
1	96 ± 2	36 ± 5	2.1	0.1
2	43 ± 5	30 ± 3	1.5	0.01
3	293 ± 12	88 ± 6	1.1	0.4

[a] NMR experiments were performed in $CDCl_3$, at $T = 298$ K. [b] $\Delta\delta_{obs} = \delta_{obs}(C_{max}) - \delta_{obs}(4\ mM)$ for the NH protons adjacent to the crown ether moiety. [c] C_{max} = maximal solubility in $CDCl_3$.

probably hindered and corresponds to a loss of conformational freedom of the macrocyclic moiety motion, which is restricted when internal hydrogen bonds form.

Calculation of the association constants of **1**−**3** revealed that for monopropylurea **2** the self-organization decreased, while for dipropylurea **3** it strongly increased (Table 1). As expected, the monopropylurea **2** is less H-bonded than benzeneurea derivative **1**, proving the importance of $\pi-\pi$ stacking in self-organization. In contrast, the dipropylurea **3** is more highly associated than **1** and **2**, indicating a strong cooperativity of the urea head-to-tail association process.

The X-ray structure of **1** described earlier[12] reveals that two adjacent macrocycles present a tight contact due to the cooperative urea H-bonding (average N−O distance of 3.01 Å) and $\pi-\pi$ stacking and the C−H$\cdots\pi$ interactions. It results in tubular superstructures with an internal van der Waals diameter of 2.72 Å and a spacing of 4.83 Å between parallel off-centered macrocycles (offset angle of 70.5°[9b]) (Figure 2a,b).

The macrocyclic heteropolysiloxanes **1**, **2**, and **3** can gelate the chloroformic solutions. To transcribe these morphological organogel superstructures of **2** and **3** into hybrid solid materials $\mathbf{M^2}$ and $\mathbf{M^3}$, we carried out sol−gel polymerization of covalently attached alkoxysilane under mild hydrolysis−condensation conditions. This represents an intermediate approach between the previously reported methods to form self-organized hybrid materials by use of TEOS organogels templation[3a,b] and appropriate silylated organic molecules.[3c,d]

Fourier transform infrared (FTIR) and NMR spectroscopic analyses demonstrate the formation of a self-assembled organic−inorganic network. Evidence for H-bond formation was obtained from the FTIR spectra: in both organogels ($C > 0.2$ M) and in the solids $\mathbf{M^2}$ and $\mathbf{M^3}$, the H-bond urea vibration shifts were detected: $\nu_{N-H} = 3320$ ($\Delta\nu = 30$), $\nu_{C=O(amideI)} = 1635$ ($\Delta\nu = 15$), and $\nu_{C-N(amideII)} = 1565$ ($\Delta\nu = 25$) cm^{-1}. After hydrolysis−condensation reactions, FTIR spectra of $\mathbf{M^2}$ and $\mathbf{M^3}$ materials showed the appearance of broad vibrations $\nu_{Si-O-Si} = 1000-1200$ cm^{-1} instead the vibrations $\nu_{Si-OEt} = 1075$, 1100, and 1170 cm^{-1} initially observed for the molecular precursors **2** and **3**. This shed light that the self-organization by hydrogen bonding of organogel superstructures was preserved in the hybrid materials throughout the inorganic polymerization process.

The ^{29}Si magic-angle spinning (MAS) NMR spectroscopic experiments agree with a progressive condensation of alkoxysilane moieties: (a) in the first step, by stirring at room temperature, a very weak connected hybrid sol was observed, mostly composed of T^1 and T^2 species; (b) the sols (or weak hydrolyzed organogels) were deposited onto microporous polymeric supports and condensed in a second step at different temperatures; (c) reticulated **M²** (79.1%) and partial condensated **M³** (28.9%) materials were prepared at 60 °C; (d) more advanced condensation of about 90% with a higher proportion of T^3 species were obtained by heating to 100 °C for both **M²** and **M³** systems, which have been found to be thermally stable up to 200 °C.

To our best knowledge, this is the first example of a hybrid nanomaterial based on bridged silsesquioxanes prepared in an aprotic solvent (chloroform), under heterogeneous catalysis (see experimental details in Supporting Information). That strategy, using the covalently linked silica precursors **2** and **3**, consists of minimizing the cross-linking reactions favored by hydrolysis and maximizing the organizing urea head-to-tail intergelator H-bonds instead of the "destructive" urea−"anionic" silica H-bonding interactions.[3,17] This allows preservation of the preorganized lamellar superstuctures of macrocyclic organogelators (see below) during the first mild-hydrolysis step, leading to further hybrid condensed species with a high degree of ordering in a polycondensation (transcription) step by thermal treatments.

Scanning electron microscopy (SEM) revealed the thin-layer films prepared at 60 °C (thickness of about 2 μm) were dense, without pinholes (Figure 3a) (see experimental details in Supporting Information). Figure 3b depicts a typical large scan area transmission electron microscopy (TEM) image of a film of **M²** and shows well-resolved details of the highly ordered uniform rows. The repeating motif is formed by discrete alternative light (inorganic siloxane matrix) and dark (organic self-assembled molecules) rows with a periodicity in one direction of about 20 Å.

A model of the molecular arrangement of **M²** can be postulated on the basis of the TEM measurements and the single-crystal X-ray analysis of compound **1** (Figure 3b,c). Several arguments support our model:

(1) The 3D crystal packing of **1** deduced from the single-crystal X-ray data[12] indicates that the structure is mainly defined by a two-dimensional (2D) periodicity of parallel sheets of about 15 Å in width resulting in the alignment of oppositely oriented macrocycles in the plane *bc*; the H-bond self-assembly of stacked H-bond macrocycles leads in addition to the propagation of macrocycles along the orthogonal direction *a* of this plane in the form of parallel polytubular arrangements of the periodic layers (Figure 3c).

(2) The length of the individual siloxane macrocyclic receptor **2** is about 21 Å (we assume a linear structure of about 15 Å for the ureido macrocyclic moiety and about 6 Å for the −C−Si−O−Si−O sequence; Figure 3b), which is consistent with the distance observed from TEM.

(3) The X-ray powder diffractograms of precursor **2** and the hybrid **M²** (Figure 4a) show that long-range three-dimensional (3D) order remains even after the condensation step, albeit less pronounced than in the precursor: there are less well-defined peaks than are present for the precursor and the peak width

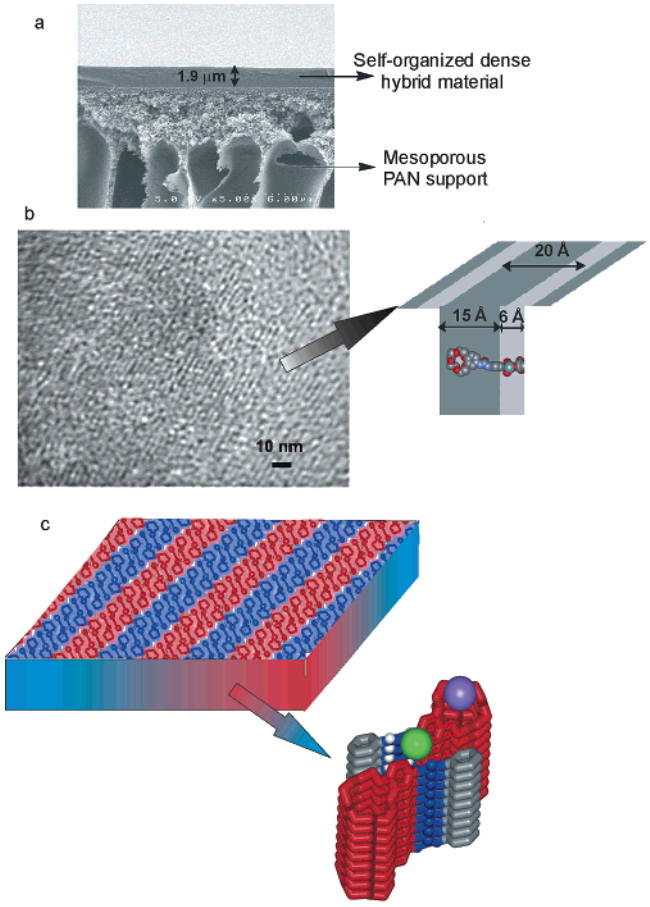

Figure 3. (a) Cross-section micrograph of membrane **M²**: the thin-layer dense film deposited onto polymeric supports. (b) TEM image of the surface and suggested model for the arrangement of hybrid material **M²**. (c) X-ray crystal packing (stick representation) of parallel sheets disposition of receptors **1** in the plane *bc* and of orthogonal tubular transport devices (direction *a*) for both cation- (violet sphere) and anion- (green sphere) assisted diffusion in macrocycles (red) and in sandwich urea- (blue) type subdevices, respectively.

increases, indicating smaller domains in which coherent scattering occurs. Peaks are observed around q = 0.27, 0.6, and 0.95 Å^{-1} ($q = (4\pi \sin \theta)/\lambda$), corresponding to interplanar distances of 23, 10, and 6.5 Å, respectively. The diffractogram of **2** could be indexed on the basis of a monoclinic unit cell with cell parameters a = 22.70 Å, b = 8.30 Å, c = 14.28 Å, α = 90°, β = 94.30°, γ = 90°, and V = 2682 Å^3 (possible space groups $P2_1$ or $P2_1/m$), such that the main diffraction peak at q = 0.27 Å^{-1} can be indexed as (100). The volume accommodates approximately the extra non-hydrogen atoms of **2** with respect to **1**.[16] It can be postulated that the three-dimensional organization of **2** is approximately equal to that of **1**, i.e., a propagation

(13) Reichwein-Buitenhuis, E. G.; Visser, H. C.; de Jong, F.; Reinhoudt, D. N. *J. Am. Chem. Soc.* **1995**, *117*, 3913−3921.
(14) The broad diffraction peaks observed in the diffractograms of **3** are related to the presence of two cis−trans isomers of the former commercial precursor.
(15) For example, the receptor **1** repeats along the crystallographic *a*-axis, but the corresponding (100) reflection is systematically absent in space group $P2_1/n$. Had the (100) reflection been present because of another space group symmetry, then the corresponding distance would still not correspond to the length of the macrocyclic receptor **1**, since the *a*-axis is about 4 Å longer.
(16) The cell volume of **1** is 2208 Å^3.[12] Replacing the phenyl group by a triethoxysilyl group gives seven extra non-hydrogen atoms. Since each non-hydrogen occupies approximately 18 Å^3, this gives for Z = 4 (space group $P2_1/m$) an extra volume of 504 Å^3 with respect to that of **1**, thus V = 2712 Å^3, close to the proposed cell volume of **2** (V = 2682 Å^3)

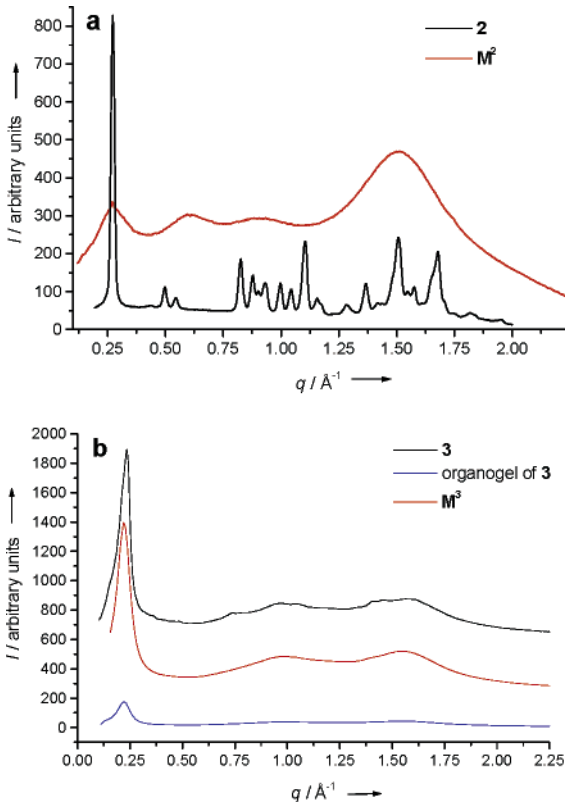

Figure 4. X-ray powder diffraction patterns of (a) precursor **2** (black) and hybrid **M²** (red) and of (b) precursor **3** (black), organogel of **3** (blue) in $CHCl_3$, and hybrid **M³** (red). I = intensity.

of macrocycles along the main direction *a*. It is noted that no single crystals suitable for full structure determination have been found. The sol−gel processes used for the preparation of the hybrids have been found to influence the organization of the materials: (a) The diffraction peak at $q = 0.27$ Å^{-1} appears broader with lower intensity, indicating a less well defined 3D long-range order in the solid **M²** hybrid (Figure 4a).

The broad peak around $q = 0.6$ Å^{-1} is not clearly related to diffraction peaks of **2**, indicating a structural rearrangement of **M²** compared to that of **2** in a different direction than the main direction defined by the first diffraction peak at $q = 0.27$ Å^{-1}. (b) The same premise hold true in the case of the precursor **3**[14] and the hybrid **M³**, which present an intense peak at $q = 0.22$ Å^{-1} corresponding to an interplanar distance of 28.5 Å. Similarly, the intensity of this peak decreases and becomes large and less defined in the organogel of **3** and in the solid hybrid **M³** (Figure 4b). (c) The very broad peaks around $q = 0.95$ Å^{-1} (**M²**) and $q = 1.5$ Å^{-1} (**M³**) are to be related to short-range order features. It is delicate to compare the *d* spacing from X-ray diffractions with that observed in the TEM image, since crystallographic symmetry could easily mask the particular distance observed in TEM analysis.[15]

The X-ray structural data and TEM analysis allow the following qualitative conclusions to be drawn:

(a) The ordered rows seen on the TEM micrograph are related to a moderate long-range order as detected by X-ray diffraction. The resulting structure of **M²** is partly related to that of precursor **1** as can be inferred from the minimal displacement of the first peak at $q = 0.27$ Å^{-1}. We assume a 2D parallel disposition of macrocyclic compounds (dark color in TEM image) alternated with parallel silica layers (light color in TEM image) (Figure 3b,c). Deviations from the directionality found in the TEM images might arise either from the unlikely distortions of organic and inorganic phases themselves or from intercalation from adjacent components or might simply indicate a grain boundary.

(b) The packing of organic macrocycles **1** by H-bonds suggests that the third main direction of periodicity generates a tubular arrangement of macrocycles in **M²** oriented in a parallel fashion along the layers and orthogonally disposed with respect to these layers.

(c) The molecular arrangement in hybrid **M²** defines a particularly attractive functional transport device that encodes the required information for both cation (tubular macrocycles) and anion (sandwich-urea) directional-diffusion transport mechanisms in the hybrid membrane material (Figure 3c). It results in continual translocation complexing pathways in a similar manner that the pore-type proteins assist ion diffusion along the cell membrane.

To demonstrate the generation of ion-pair translocation pathways into synthesized membranes, we carried out transport experiments. The membrane performances depend and are based on encoded molecular features of heteroditopic precursors and are designed to transport ion pairs. The ATP^{2-} transport across these membranes according to the above directional-diffusion transport mechanism and against its thermodynamic gradient was evaluated under passive and ion-driven pumping conditions. Passive transport of highly hydrophilic ATP^{2-} through **M²** and **M³** was not observed when the feed phase was filled with a 10^{-3} M solution of ATP^{2-}, while the strip phase was distilled water. In this case, the ATP^{2-} transport cannot be driven by concentration gradients, probably due to its lower partitioning at the feed/membrane interface. For this reason we have studied an active transport approach: experiments have been conducted with concentrated NaCl in the feed solution in order to investigate the ATP^{2-} transfer driven by Na^+ gradients.

The self-organized **M²** and **M³** presented nonlinear saturation behavior of initial Na^+ permeability P_0 (Figure 5a), indicating a strong affinity of the membrane for the solute. The partition of Na^+ was higher at the strip solution interface than at the feed solution interface ($K^f/K^s = 0.2$); thus its transport is simply "amplified". This is consistent with the development of ion-conducting pathways along membrane-spanning self-organized "frozen" oligomers.

Figure 5b shows the concentration versus time transport profiles by **M³** when the initial concentrations of the ATP^{2-} both in the feed and in the strip solutions are 10^{-3} M, while the NaCl concentration in the feed phase is 10^{-1} M. We first noted a strong transport of the Na^+ ion across the membrane from the feed to the strip solutions. This induced an opposite (negative) membrane potential (ϵ), which slowed the diffusion of Na^+ ions and accelerated the negative ones (Figure 5c). The resulting effect is a temporary (25 h), quite remarkable ATP^{2-} pumping (~45%) against its concentration gradient from the feed to the strip solution. This unusual behavior can be rationalized by considering the large charged ATP^{2-} anions as "active spectators" of the diffusion events of more concentrated

(17) Since this paper was submitted, two other articles have been published reporting the synthesis of self-assembled silylated organogels: (a) Dautel, O. J.; Lère-Porte, J. P.; Moreau, J. J.; Wong, C.-M. M. *Chem. Commun.* **2003**, 2662−2663. (b) Moreau, J. J.; Pichon, B. P.; Wong, C.-M. M.; Bied, C.; Pritzkow, H.; Bantignes, J. L.; Dieudonné, P.; Sauvajol, J. L. *Angew. Chem., Int. Ed.* **2004**, *43*, 203−206.

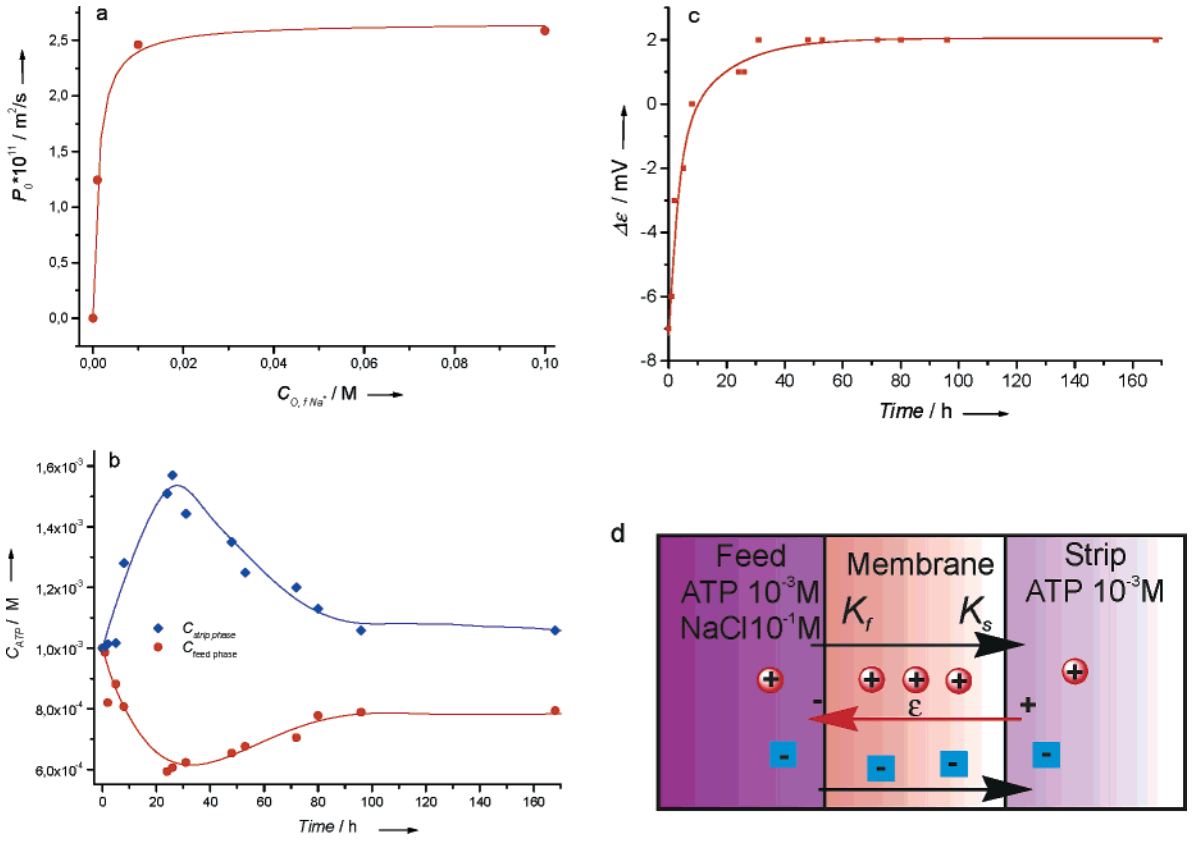

Figure 5. Membrane transport results of ATP^{2-} and Na^+ by **M**[2] hybrid material. (a) Permeability P_0 versus initial Na^+ concentration C_0 dependence. (b, c) Concentration and membrane potential versus time transport profiles of the ATP^{2-}. (d) Proposed Na^+-powered pumping mechanism of the ATP^{2-} against its concentration gradient.

and smaller Na^+ and Cl^- partners.[18] After ~25 h the Na^+ transport stopped and the membrane potential became positive and constant (Figure 5b). At this point the pumping stopped and the ATP^{2-} was transported back by concentration gradient from the strip to the feed solution, approximately reaching the initial equilibrium conditions.

Conclusion

Controlled formation of the three-dimensional functional devices in silica make hybrid materials of interest for the development of a new supramolecular approach to nanoscience and nanotechnology through self-organization, toward systems of increasing behavioral and functional addressability (catalysis, optic and electronic applications, etc.).

The above results describe a simple synthetic hybrid material that successfully formed transport patterns so as to enable efficient translocation events. To our knowledge, the present system is the first example of a hybrid nanomaterial where the concept of self-organization and a specific function (generation of specific translocation pathways in a hybrid solid) might in principle be associated. This system has been employed successfully to design a *solid dense membrane*, functioning as an ion-powered ATP^{2-} pump, and illustrates how a self-organized hybrid material performs interesting and potentially useful functions.

Acknowledgment. This paper is dedicated to Professor Louis Cot. This research was supported by CNRS and Ministère de la Recherche et de la Technologie, ACI Jeunes Chercheurs 4034, 2002. We also thank Dr. Nadine Hovnanian for ^{29}Si NMR and X-ray powder diffraction measurements and Mr. L Datas for TEM analysis.

Supporting Information Available: Experimental procedures (PDF). This information is available free of charge via the Internet at http://pubs.acs.org.

JA039146Z

(18) This is related to a similar proton-driven ion pump. Palmeri, J., unpublished results.